Transient Simulation of Magnetic Circuits Using the Permeance-Capacitance Analogy

Jost Allmeling
Plexim GmbH
Technoparkstrasse 1
8005 Zurich, Switzerland
Email: allmeling@plexim.com

Wolfgang Hammer
Plexim GmbH
Technoparkstrasse 1
8005 Zurich, Switzerland
Email: hammer@plexim.com

John Schönberger
TridonicAtco Schweiz AG
Obere Allmeind 2
8755 Ennenda, Switzerland
Email: john.schoenberger@tridonic.com

***Abstract*—When modeling magnetic components, the permeance-capacitance analogy avoids the drawbacks of traditional equivalent circuits models. The magnetic circuit structure is easily derived from the core geometry, and the energy relationship between electrical and magnetic domain is preserved. Non-linear core materials can be modeled with variable permeances, enabling the implementation of arbitrary saturation and hysteresis functions. Frequency-dependent losses can be realized with resistors in the magnetic circuit.**

The magnetic domain has been implemented in the simulation software PLECS. To avoid numerical integration errors, Kirchhoff's current law must be applied to both the magnetic flux and the flux-rate when solving the circuit equations.

I. Introduction

Inductors and transformers are key components in modern power electronic circuits. Compared to other passive components they are difficult to model due to the non-linear behavior of magnetic core materials and the complex structure of components with coupled windings.

This paper compares different approaches to model magnetic components by means of equivalent circuits with lumped elements. It highlights the advantages of the permeance-capacitance analogy over the traditional coupled-inductor model and the reluctance-resistance analogy.

With the permeance-capacitance analogy, saturable cores are modeled as variable permeances. A method for modeling a saturable core using a continuously-variable permeance is described. The saturable core model can be extended to model frequency-depending losses and hysteresis.

Finally, the implementation of the magnetic domain in the commercial simulation software PLECS is described. The system equations must be set up by applying Kirchhoff's current law to both flux-rate and flux in order to avoid numerical integration errors.

II. Equivalent circuits for magnetic components

To model complex magnetic structures with equivalent circuits, three different approaches exist: Coupled inductors, the resistance-reluctance analogy and the capacitance-permeance analogy.

978-1-4244- 9373-9/12/$26.00 ©2012 IEEE

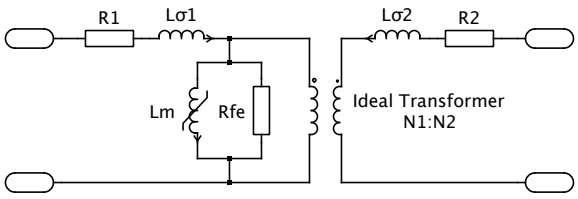

Fig. 1. Transformer implementation with coupled inductors

A. Coupled inductors

In the coupled inductor approach, the magnetic component is modeled directly in the electrical domain as an equivalent circuit, in which inductances represent magnetic flux paths and losses incur at resistors. Magnetic coupling between windings is realized either with mutual inductances or with ideal transformers.

Using coupled inductors, magnetic components can be implemented in any circuit simulator since only electrical components are required. This approach is most commonly used for representing standard magnetic components such as transformers. Fig. 1 shows an example for a two-winding transformer, where $L_{\sigma 1}$ and $L_{\sigma 2}$ represent the leakage inductances, L_{m} the non-linear magnetization inductance and R_{fe} the iron losses. The copper resistances of the windings are modeled with R_1 and R_2.

However, the equivalent circuit bears little resemblance to the physical structure of the magnetic component. For example, parallel flux paths in the magnetic structure are modeled with series inductances in the equivalent circuit. For non-trivial magnetic components such as multiple-winding transformers or integrated magnetic components, the equivalent circuit can be difficult to derive and understand. In addition, equivalent circuits based on inductors are impossible to derive for non-planar magnetic components [4].

B. Reluctance-resistance analogy

The traditional approach to model magnetic structures with equivalent electrical circuits is the reluctance-resistance analogy. The magnetomotive force (mmf) F is regarded as analogous to voltage and the magnetic flux Φ as analogous to current. As a consequence, magnetic reluctance of the flux

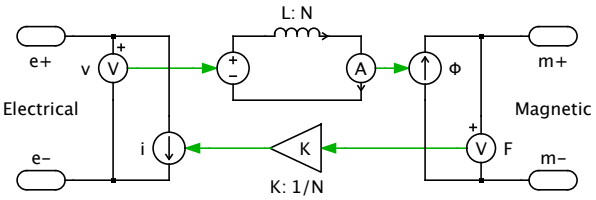

Fig. 2. Implementation of magnetic interface

path $\mathcal{R}$ corresponds to electrical resistance:

$$\mathcal{R} = \frac{\mathcal{F}}{\Phi} \tag{1}$$

The magnetic circuit is simple to derive from the core geometry: Each section of the flux path is represented by a reluctance and each winding becomes an mmf source.

To link the external electrical circuit with the magnetic circuit, a magnetic interface is required [1]. The magnetic interface represents a winding and establishes a relationship between flux and mmf in the magnetic circuit and voltage v and current i at the electrical ports:

$$v = N\frac{\mathrm{d}\Phi}{\mathrm{d}t} \tag{2}$$

$$i = \frac{F}{N} \tag{3}$$

where N is the number of turns. If the magnetic interface is implemented with an integrator it can be solved by an ODE solver:

$$\Phi = \frac{1}{N}\int v\,\mathrm{d}t \tag{4}$$

Fig. 2 outlines a possible implementation of the magnetic interface in a circuit simulation software.

Although the reluctance-resistance duality may appear natural and is widely accepted, it is an inferior choice for multiple reasons:

- Physically, energy is stored in the magnetic field of a volume unit. In a magnetic circuit model with lumped elements, the reluctances should therefore be storage components. However, with the traditional choice of mmf and flux as magnetic system variables, reluctances are modeled as resistors, i.e. components that would usually dissipate energy. It is also confusing that the magnetic interface is a storage component.
- To model energy dissipation in the core material, inductors must be employed in the magnetic circuit, which is even less intuitive.
- Magnetic circuits with non-linear reluctances generate differential-algebraic equations (DAE) resp. algebraic loops that cannot be solved with ODE solvers for ordinary differential equations.
- The use of magnetic interfaces results in very stiff system equations for closely coupled windings.

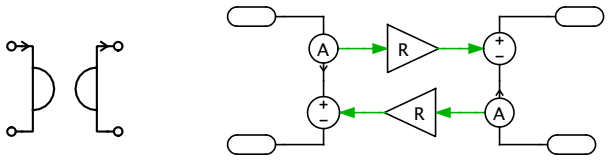

Fig. 3. Gyrator symbol and implementation

C. Permeance-capacitance analogy

To avoid the drawbacks of the reluctance-resistance analogy the authors are advocating the alternative permeance-capacitance analogy [2]–[5]. Here, the mmf F is again the across-quantity (analogous to voltage), while the *rate-of-change* of magnetic flux $\dot{\Phi}$ is the through-quantity (analogous to current). With this choice of system variables, magnetic permeance $\mathcal{P}$ corresponds to capacitance:

$$\dot{\Phi} = \mathcal{P}\,\frac{\mathrm{d}F}{\mathrm{d}t} \tag{5}$$

Hence it is convenient to use permeance $\mathcal{P}$ instead of the reciprocal reluctance $\mathcal{R}$ to model flux path elements. Because permeance is modeled with storage components, the energy relationship between the actual and equivalent magnetic circuit is preserved. The permeance value of a volume element is given by

$$\mathcal{P} = \frac{1}{\mathcal{R}} = \frac{\mu_0\mu_\mathrm{r}A}{l} \tag{6}$$

where $\mu_0 = 4\pi \times 10^{-7}\,\mathrm{N/A^2}$ is the magnetic constant, μ_r is the relative permeability of the material, A is the cross-sectional area and l the length of the flux path.

Dissipator components (analogous to electrical resistors) can be used in the magnetic circuit to model losses. They can be connected in series or in parallel to a permeance component, depending on the nature of the specific loss. The energy relationship is maintained as the power

$$P_\mathrm{loss} = F\,\dot{\Phi} \tag{7}$$

converted into heat in a dissipator corresponds to the power lost in the electrical circuit.

Windings form the interface between the electrical and the magnetic domain. A winding of N turns is described with the equations below. The left-hand side of the equations refers to the electrical domain, the right-hand side to the magnetic domain.

$$v = N\dot{\Phi} \tag{8}$$

$$i = \frac{F}{N} \tag{9}$$

Because a winding converts through-quantities ($\dot{\Phi}$ resp. i) in one domain into across-quantities (v resp. F) in the other domain, it can be implemented with a gyrator, in which N is the gyrator resistance R [5]. Fig. 3 shows the symbol for a gyrator and its implementation in the simulation software PLECS.

The gyrator component could be used with regular capacitors to build magnetic circuits. However, neither the gyrator

symbol nor the capacitor adequately resemble a winding respectively a flux path. Moreover, any direct connection between the electrical and magnetic domain made by mistake would lead to non-causal systems that are very difficult to debug. Therefore, dedicated magnetic components should be used when modeling magnetic circuits.

III. Magnetic circuit domain in PLECS

The permeance-capacitance analogy has been implemented in PLECS by means of a special domain. The available magnetic components include windings, constant and variable permeances as well as dissipators. By connecting them according to the physical structure the user can create equivalent circuits for arbitrary magnetic components. The transformer in Fig. 1 appears as shown in Fig. 4 when modeled in the magnetic domain.

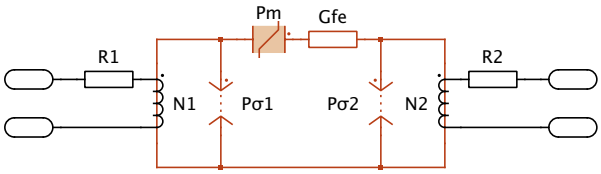

Fig. 4. Transformer implementation in the magnetic domain

$\mathcal{P}_{\sigma 1}$ and $\mathcal{P}_{\sigma 2}$ represent the linear permeances of the leakage flux path, $\mathcal{P}_{\mathrm{m}}$ the saturable permeance of the core, and G_{fe} dissipates the iron losses. The winding resistances R_1 and R_2 are modeled in the electrical domain.

A. Modeling non-linear magnetic material

Non-linear magnetic material properties such as saturation and hysteresis can be modeled using the variable permeance component. The permeance is determined by the signal fed into the input of the component. The flux-rate through a variable permeance $\mathcal{P}(t)$ is governed by the equation

$$\dot{\Phi} = \frac{\mathrm{d}}{\mathrm{d}t}\left(\mathcal{P}\cdot F\right) = \mathcal{P}\cdot\frac{\mathrm{d}F}{\mathrm{d}t} + \frac{\mathrm{d}}{\mathrm{d}t}\mathcal{P}\cdot F \tag{10}$$

F is the state variable, and hence (10) must be solved for $\frac{\mathrm{d}F}{\mathrm{d}t}$. Therefore, the control signal must provide the values of both $\mathcal{P}(t)$ and $\frac{\mathrm{d}}{\mathrm{d}t}\mathcal{P}(t)$.

When specifying the characteristic of a non-linear permeance, we need to distinguish carefully between the *total* permeance $\mathcal{P}_{\mathrm{tot}}(F) = \Phi/F$ and the *differential* permeance $\mathcal{P}_{\mathrm{diff}}(F) = \mathrm{d}\Phi/\mathrm{d}F$.

If the *total* permeance $\mathcal{P}_{\mathrm{tot}}(F)$ is known the flux-rate $\dot{\Phi}$ through a time-varying permeance is calculated as

$$\begin{aligned}\dot{\Phi} &= \frac{\mathrm{d}\Phi}{\mathrm{d}t}\\ &= \frac{\mathrm{d}}{\mathrm{d}t}\left(\mathcal{P}_{\mathrm{tot}}\cdot F\right)\\ &= \mathcal{P}_{\mathrm{tot}}\cdot\frac{\mathrm{d}F}{\mathrm{d}t} + \frac{\mathrm{d}\mathcal{P}_{\mathrm{tot}}}{\mathrm{d}t}\cdot F\\ &= \mathcal{P}_{\mathrm{tot}}\cdot\frac{\mathrm{d}F}{\mathrm{d}t} + \frac{\mathrm{d}\mathcal{P}_{\mathrm{tot}}}{\mathrm{d}F}\cdot\frac{\mathrm{d}F}{\mathrm{d}t}\cdot F\\ &= \left(\mathcal{P}_{\mathrm{tot}} + \frac{\mathrm{d}\mathcal{P}_{\mathrm{tot}}}{\mathrm{d}F}\cdot F\right)\cdot\frac{\mathrm{d}F}{\mathrm{d}t}\end{aligned} \tag{11}$$

In this case, the control signal for the variable permeance component is

$$\begin{bmatrix}\mathcal{P}(t)\\ \frac{\mathrm{d}}{\mathrm{d}t}\mathcal{P}(t)\end{bmatrix} = \begin{bmatrix}\mathcal{P}_{\mathrm{tot}} + \frac{\mathrm{d}}{\mathrm{d}F}\mathcal{P}_{\mathrm{tot}}\cdot F\\ 0\end{bmatrix} \tag{12}$$

In most cases, however, the *differential* permeance $\mathcal{P}_{\mathrm{diff}}(F)$ is provided to characterize magnetic saturation and hysteresis. With

$$\begin{aligned}\dot{\Phi} &= \frac{\mathrm{d}\Phi}{\mathrm{d}t}\\ &= \frac{\mathrm{d}\Phi}{\mathrm{d}F}\cdot\frac{\mathrm{d}F}{\mathrm{d}t}\\ &= \mathcal{P}_{\mathrm{diff}}\cdot\frac{\mathrm{d}F}{\mathrm{d}t}\end{aligned} \tag{13}$$

the control signal is

$$\begin{bmatrix}\mathcal{P}(t)\\ \frac{\mathrm{d}}{\mathrm{d}t}\mathcal{P}(t)\end{bmatrix} = \begin{bmatrix}\mathcal{P}_{\mathrm{diff}}\\ 0\end{bmatrix} \tag{14}$$

B. Saturation curves for soft-magnetic material

Curve fitting techniques can be employed to model the properties of ferromagnetic material. Here, two functions for modeling the non-linear primary saturation curve in soft magnetic materials are presented.

1) coth fit: The first function, referred to as the coth fit, was adapted from the Langevian equation for bulk magnetization without interdomain coupling [6]–[8] and is given as follows:

$$B = B_{\mathrm{sat}}\left(\coth\frac{3H}{a} - \frac{a}{3H}\right) + \mu_{\mathrm{sat}}H \tag{15}$$

Calculating the derivate of B with respect to H yields:

$$\frac{\mathrm{d}B}{\mathrm{d}H} = B_{\mathrm{sat}}\left(\frac{\tanh^2\left(H/a\right)-1}{a\,\tanh^2\left(H/a\right)} - \frac{a}{H^2}\right) + \mu_{\mathrm{sat}} \tag{16}$$

2) atan fit: The second function, referred to as the atan fit, has been proposed in [9]:

$$B = \frac{2}{\pi}B_{\mathrm{sat}}\tan^{-1}\left(\frac{\pi H}{2a}\right) + \mu_{\mathrm{sat}}H \tag{17}$$

$$\frac{\mathrm{d}B}{\mathrm{d}H} = \frac{B_{\mathrm{sat}}}{a\left(1+\left(\frac{\pi}{2}H/a\right)^2\right)} + \mu_{\mathrm{sat}} \tag{18}$$

Both fitting functions have three degrees of freedom which are set by the coefficients μ_{sat}, B_{sat} and a. μ_{sat} is the fully saturated permeability, which is usually

$$\mu_{\mathrm{sat}} = \mu_0 \tag{19}$$

B_{sat} defines the knee of the saturation transition between unsaturated and saturated permeability as illustrated in Fig. 5:

$$B_{\mathrm{sat}} = \left(B - \mu_{\mathrm{sat}}H\right)\Big|_{H\to\infty} \tag{20}$$

The coefficient a can be determined using the unsaturated permeability μ_{unsat} at $H = 0$:

$$a = B_{\mathrm{sat}} / \left(\mu_{\mathrm{unsat}} - \mu_{\mathrm{sat}}\right) \tag{21}$$

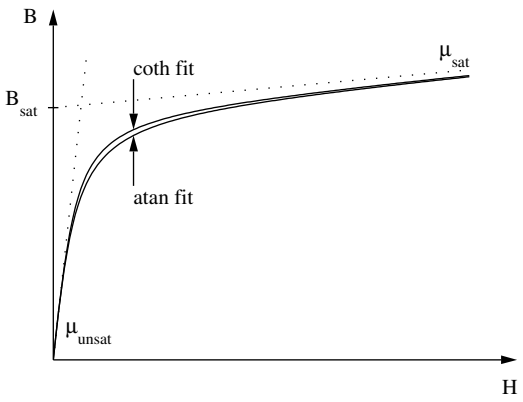

Fig. 5. Saturation characteristics of coth and atan fitting functions

Fig. 5 illustrates the saturation characteristics for both fitting functions. The saturation curves differ only around the transition between unsaturated and saturated permeability. The coth fit expresses a slightly tighter transition.

With the relationships $\Phi = B \cdot A$ and $F = H \cdot l$ the control signal $\mathcal{P}_{\mathrm{diff}}$ for the variable permeance is easily derived from (16) and (18).

C. Hysteresis model

To account for hysteresis effects in ferro-magnetic material, a scalar Preisach model with a Lorentzian distribution function [10] has been employed to establish a non-linear relationship between the magnetic field strength H and the flux density B. For this model, Fig. 6 shows a fully excited major hysteresis curve starting with the virgin curve and including some minor reversal loops. The major curve is defined by the saturation point (H_{sat}, B_{sat}), the coercitive field strength H_{c}, the remanence flux density B_{r} and the saturated permeability μ_{sat}.

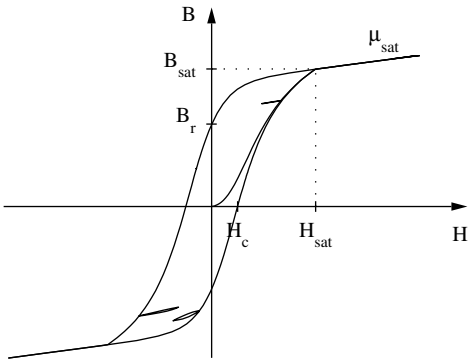

Fig. 6. Hysteresis curve of Preisach model with Lorentzian distribution function

Since the Preisach model is static, the shape of the hysteresis curve is independent of the applied frequency. To include e.g. frequency-dependent eddy current losses, a dissipator must be connected in series to the permeance as shown in Fig. 4.

D. Solving magnetic circuit equations

The system equations of the equivalent circuit are determined by Kirchhoff's current and voltage laws. At each node, the sum of directed flux-rates in all branches n is zero:

$$\sum_{k=1}^{n} \dot{\Phi}_k = 0 \tag{22}$$

Around any closed circuit loop, the directed sum of the mmf is zero:

$$\sum_{k=1}^{n} F_k = 0 \tag{23}$$

However, since Kirchhoff's current law was not applied to the magnetic flux itself, Gauss's law of magnetism

$$\oiint_{\partial V} B \cdot \mathrm{d}A = 0 \tag{24}$$

would be violated, if

- the sum of all directed fluxes at simulation start was not zero, or
- an error accumulated during the numerical integration.

Therefore, the solver needs to enforce Kirchhoff's current law for the flux

$$\sum_{k=1}^{n} \Phi_k = 0 \tag{25}$$

explicitly. In case of linear systems with constant permeances $\mathcal{P}_k$, this can simply be achieved by including

$$\sum_{k=1}^{n} \Phi_k = \sum_{k=1}^{n} \mathcal{P}_k \cdot F_k = 0 \tag{26}$$

in the system equations.

To solve circuits with variable permeances $\mathcal{P}_k(t)$ the residual flux Φ_{res} must be computed for every node

$$\Phi_{\mathrm{res}} = \sum_{k=1}^{n} \Phi_k(F_k, t) \stackrel{!}{=} 0 \tag{27}$$

and minimized by adjusting F_k. For all variable permeances the flux Φ_k must be provided. Thus, the input signal of a saturable permeance becomes:

$$\begin{bmatrix} \mathcal{P}(t) \\ \frac{\mathrm{d}}{\mathrm{d}t}\mathcal{P}(t) \\ \Phi(t) \end{bmatrix} = \begin{bmatrix} \mathcal{P}_{\mathrm{diff}} \\ 0 \\ \mathcal{P}_{\mathrm{tot}} \cdot F \end{bmatrix} = \begin{bmatrix} \mathcal{P}_{\mathrm{tot}} + \frac{\mathrm{d}}{\mathrm{d}F}\mathcal{P}_{\mathrm{tot}} \cdot F \\ 0 \\ \mathcal{P}_{\mathrm{tot}} \cdot F \end{bmatrix} \tag{28}$$

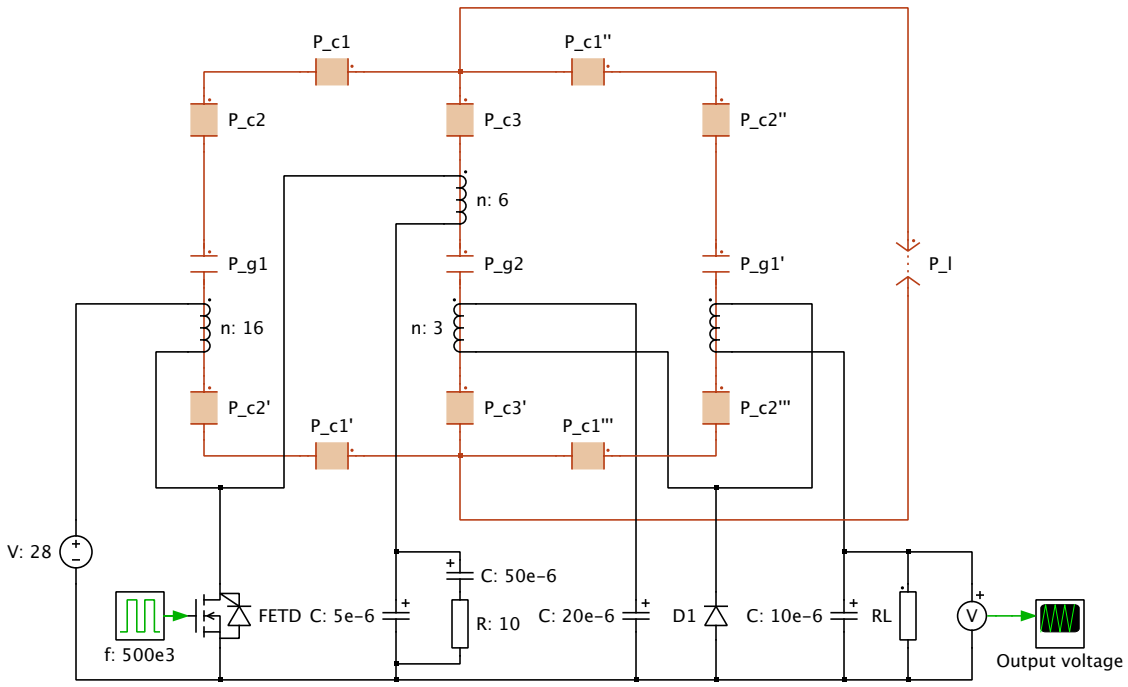

Fig. 7. Isolated Ćuk converter with integrated magnetics modeled in PLECS

IV. Application Example: Ćuk Converter

To demonstrate the feasibility of the proposed approach, an isolated Ćuk converter with integrated magnetics [4] has been modeled in PLECS (Fig. 7). Due to proper magnetic coupling between the windings, this Ćuk converter operates with zero ripple in both the input and output current.

The magnetic circuit consists of two opposing E-cores spaced by an air gap $\mathcal{P}_{gn}$. Each geometric section of the core is modeled as a separate permeance $\mathcal{P}_{cn}$. The leakage fluxes are bundled and simplified to a single flux path $\mathcal{P}_{\mathrm{l}}$.

Fig. 8 shows the simulation results for linear core permeances with a relative permeability $\mu_{\mathrm{r}} = 2000$. As expected, the current ripple in the output winding is negligible. It has been verified, that the flux in the three core legs and the stray

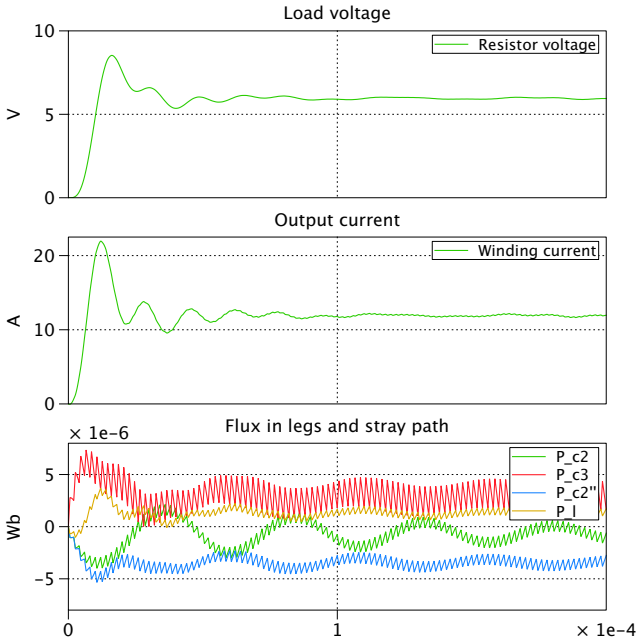

Fig. 8. Simulation results for isolated Ćuk converter with linear core

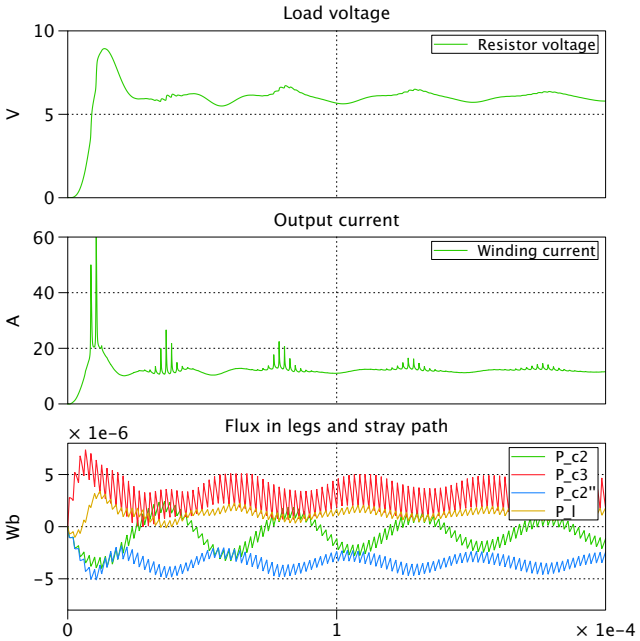

Fig. 9. Simulation results for isolated Ćuk converter with saturable core

flux indeed add up to zero.

The results in Fig. 9 were obtained by replacing all linear core permeances with saturable permeances using the atan fit. The saturation flux density was set to $B_{\mathrm{sat}} = 0.4\,\mathrm{T}$ and the saturated relative permeability to $\mu_{\mathrm{r,sat}} = 1$. The unsaturated relative permeability was left at $\mu_{\mathrm{r,unsat}} = 2000$.

In Fig. 9 the spikes in the output current resulting from core saturation can be observed clearly. The spikes occur when the magnetic flux in the output leg $\mathcal{P}_{\mathrm{c}2''}$ (blue graph) gets close to $-5\,\mu\mathrm{Wb}$.

V. Conclusions

The permeance-capacitance analogy implemented in PLECS provides a powerful modeling domain for magnetic circuits. The structure of the magnetic circuit can be derived easily from the core geometry. Any non-linear characteristic of the core material can be modeled using the variable permeance component. By applying Kirchhoff's current law to both the flux-rate and the flux itself, the solver can integrate the magnetic circuit equations without accumulating numerical errors.

References

[1] S. El-Hamamsy and E. Chang, "Magnetics modeling for computer-aided design of power electronics circuits," in *Power Electronics Specialists Conference*, vol. 2, pp. 635–645, 1989.

[2] R. W. Buntenbach, "Improved circuit models for inductors wound on dissipative magnetic cores," in *Proc. 2nd Asilomar Conf. Circuits Syst.*, Pacific Grove, CA, Oct. 1968, pp. 229–236 (IEEE Publ. No. 68C64-ASIL).

[3] R. W. Buntenbach, "Analogs between magnetic and electrical circuits," in *Electron. Products*, vol. 12, pp. 108–113, 1969.

[4] D. Hamill, "Lumped equivalent circuits of magnetic components: the gyrator-capacitor approach," in *IEEE Transactions on Power Electronics*, vol. 8, pp. 97–103, 1993.

[5] D. Hamill, "Gyrator-capacitor modeling: A better way of understanding magnetic components," in *APEC Conference Proceedings* pp. 326–332, 1994.

[6] D. C. Jiles and D. L. Atherton, "Ferromagnetic hysteresis," in *IEEE Transactions on Magnetics*, vol. 19, no. 5, pp. 2183–2185, 1983.

[7] D. C. Jiles and D. L. Atherton, "Theory of ferromagnetic hysteresis," in *Journal of Applied Physics*, vol. 55, no. 6, pp. 2115–2120, 1984.

[8] D. C. Jiles, J. B. Thoelke and M. K. Devine, "Numerical determination of hysteresis parameters for the modeling of magnetic properties using the theory of ferromagnetic hysteresis," in *IEEE Trans. on Magnetics*, vol. 28, no. 1, pp. 27–35, 1992.

[9] C. Perez-Rojas, "Fitting saturation and hysteresis via arctangent functions," in *IEEE Power Engineering Review*, vol. 20, no. 1, pp. 55–57, 2000.

[10] B. Azzerboni, E. Cardelli, G. Finocchio and F. La Foresta, "Remarks about Preisach function approximation using Lorentzian function and its identification for nonoriented steels" in *IEEE Trans. on Magnetics*, vol. 39, no. 5, pp. 3028–3030, 2003.